

## FTIR Evidence That the PsbP Extrinsic Protein Induces Protein Conformational Changes around the Oxygen-Evolving Mn Cluster in Photosystem II<sup>†</sup>

Megumi Tomita,<sup>‡</sup> Kentaro Ifuku,<sup>§</sup> Fumihiko Sato,<sup>§</sup> and Takumi Noguchi<sup>\*‡</sup>

<sup>‡</sup>*Institute of Materials Science, University of Tsukuba, Tsukuba, Ibaraki 305-8573, Japan, and* <sup>§</sup>*Graduate School of Biostudies, Kyoto University, Kyoto 606-8502, Japan*

Received April 13, 2009; Revised Manuscript Received June 3, 2009

**ABSTRACT:** Extrinsic proteins of photosystem II (PSII) regulate the oxygen-evolving reaction performed at the Mn cluster by controlling the binding properties of the indispensable cofactors  $\text{Ca}^{2+}$  and  $\text{Cl}^-$ . However, the molecular mechanism underlying this regulation is not yet understood. We have investigated the structural couplings of the extrinsic proteins PsbO, PsbP, and PsbQ of higher plants with the Mn cluster using Fourier transform infrared (FTIR) spectroscopy. Light-induced FTIR difference spectra upon the  $\text{S}_1 \rightarrow \text{S}_2$  transition were measured using spinach PSII membranes, and the effects of the selective depletion of extrinsic proteins were examined. Depletion of the PsbP and PsbQ proteins by NaCl washing revealed clear changes in the amide I bands with no appreciable changes in the bands of carboxylate and imidazole groups, whereas the depletion of all three proteins by  $\text{CaCl}_2$  washing did not cause further changes. The original amide I features were recovered by reconstitution of the NaCl-washed PSII with PsbP, and the same recovery was observed with  $^{13}\text{C}$ -labeled PsbP. These results indicate that the PsbP protein, but not PsbQ and PsbO, affects the protein conformation around the Mn cluster in the intrinsic proteins without changing the ligand structure. Reconstitution with  $\Delta 15$ -PsbP, in which the 15 N-terminal residues were truncated, did not restore the amide I bands, indicating that the interaction of the N-terminal region induces the conformational changes. This observation correlates well with a previous finding that  $\Delta 15$ -PsbP did not restore the  $\text{Ca}^{2+}$  and  $\text{Cl}^-$  retention ability upon rebinding to PSII [Ifuku, K., et al. (2005) *Photosynth. Res.* 84, 251–255]. Therefore, the evidence strongly suggests that protein conformational changes around the Mn cluster induced by PsbP through its N-terminal region affect the binding properties of  $\text{Ca}^{2+}$  and  $\text{Cl}^-$  and enhance their retention.

Oxygen evolution by plants and cyanobacteria is performed at the oxygen-evolving center (OEC)<sup>1</sup> in the photosystem II (PSII) protein complex (1–4). X-ray crystallographic structures of the PSII core complexes from *Thermosynechococcus elongatus* at 2.9–3.5 Å resolution (5–7), together with information from EXAFS studies (8), have revealed that the OEC consists of a metal cluster of four Mn ions and one  $\text{Ca}^{2+}$  ion (the Mn cluster) and the surrounding amino acid ligands provided by the D1 and CP43 proteins. Recent crystallographic studies have demonstrated that one or two  $\text{Cl}^-$  ions are bound near the Mn cluster at a distance of 6–7 Å (7, 9). Because of the limited resolution and possible damage by X-ray radiation (10, 11), however, details of the OEC structure remain poorly understood. In the OEC, two water molecules are converted into one molecular oxygen and

four protons through a light-driven cycle consisting of five intermediates called  $\text{S}_i$  states ( $i = 0–4$ ) (1–4). Among them, the  $\text{S}_1$  state is the most dark-stable, and flash illumination advances each S state to the next as  $\text{S}_1 \rightarrow \text{S}_2 \rightarrow \text{S}_3\text{--}[\text{S}_4] \rightarrow \text{S}_0 \rightarrow \text{S}_1$ . Molecular oxygen is released during the  $\text{S}_3\text{--}[\text{S}_4] \rightarrow \text{S}_0$  transition after the transient  $\text{S}_4$  state.

The PSII complex possesses several extrinsic proteins on its lumenal side (12–16). Higher plants have three major extrinsic proteins, PsbO, PsbP, and PsbQ, which are also termed the 33, 23, and 17 kDa proteins, respectively, from their apparent molecular masses. The PsbO protein exists in all types of oxygenic photosynthetic organisms, including cyanobacteria and red algae, and is strongly associated with the PSII core complex. X-ray structures of cyanobacterial PSII complexes and cross-linking experiments have revealed that PsbO interacts directly with the CP47, CP43, D1, and D2 proteins (13, 15). PsbO functions to stabilize the Mn cluster and retain  $\text{Cl}^-$  (12, 13). The depletion of PsbO significantly retards the  $\text{S}_3\text{--}[\text{S}_4] \rightarrow \text{S}_0$  transition (17).

In contrast to PsbO, the PsbP and PsbQ proteins are replaced by the PsbV and PsbU proteins in cyanobacteria (12–15). Although PsbP-like and PsbQ-like proteins have been identified in cyanobacterial PSII complexes, they are lipoproteins with

<sup>†</sup>This study was supported by Grants-in-Aid for Scientific Research from the Ministry of Education, Culture, Sports, Science and Technology to T.N. (17GS0314 and 21370063), to K.I. and F.S. (17051016), and to K.I. (18770032).

<sup>\*</sup>To whom correspondence should be addressed. Phone: +81-29-853-5126. Fax: +81-29-853-4490. E-mail: tnoguchi@ims.tsukuba.ac.jp.

<sup>1</sup>Abbreviations: FTIR, Fourier transform infrared; Mes, 2-(*N*-morpholino)ethanesulfonic acid; PSII, photosystem II; OEC, oxygen-evolving center; SDS–PAGE, sodium dodecyl sulfate–polyacrylamide gel electrophoresis.

binding properties that are significantly different from those of plant PsbP and PsbQ (14), and they were also absent from the PSII complexes from *T. elongates* used for crystallization (5–7, 9). A low-resolution structure of plant PSII complexes obtained by electron cryomicroscopy was used to predict that PsbP interacts with the luminal surface in the vicinity of CP43 and with PsbO, and PsbQ bridges the PsbP and PsbO proteins (18). This is consistent with biochemical observations that PsbO is necessary for the stable binding of PsbP and that PsbP is required for PsbQ binding (19, 20). However, the exact locations of the PsbP and PsbQ proteins and the interactions with intrinsic proteins in the PSII complexes remain to be clarified.

The PsbP and PsbQ proteins aid in  $\text{Ca}^{2+}$  and  $\text{Cl}^-$  retention in the OEC. The depletion of PsbP and PsbQ changes the binding properties of  $\text{Ca}^{2+}$  and  $\text{Cl}^-$  depending on the S state (21, 22). In the absence of these proteins, nonphysiological concentrations of  $\text{Ca}^{2+}$  and  $\text{Cl}^-$  are required to support high  $\text{O}_2$ -evolving rates (23, 24), and  $\text{Ca}^{2+}$  is released readily from the Mn cluster during illumination (25). In addition, PsbP and PsbQ play a role in protecting the Mn cluster from exogenous reductants (26). An in vivo characterization study of PsbP and PsbQ in transgenic tobacco, in which the levels of these proteins were downregulated by RNAi, demonstrated that PsbP, but not PsbQ, was essential for maintaining PSII activity (27). *Arabidopsis* studies using RNAi have also shown that PsbP is required for the assembly and stability of PSII (28), but a PsbQ-deficient mutant was indistinguishable from the wild type under normal light conditions (29). However, the mutant could not grow photoautotrophically under low-light conditions (29).

Thus, the extrinsic proteins play important roles in optimizing oxygen evolving activity by stabilizing the Mn cluster and retaining  $\text{Ca}^{2+}$  and  $\text{Cl}^-$  cofactors. In spite of extensive biochemical and physiological studies of the extrinsic proteins in PSII, the molecular mechanisms of their functions are poorly understood.

To address this question, in this study we investigated the structural couplings of the extrinsic proteins of higher plants with the OEC using light-induced Fourier transform infrared (FTIR) difference spectroscopy. FTIR difference spectroscopy is a powerful method for detecting subtle structural changes coupled to the OEC reactions, including changes in the conformations of protein main chains, amino acid side chains, the core structure of the Mn cluster, and substrate and functional water molecules (30–35). PSII membranes from spinach were used to examine the effects of selective depletion of the extrinsic proteins by salt washes and reconstitution with PsbP on the FTIR difference spectra upon the  $\text{S}_1 \rightarrow \text{S}_2$  transition. The effect of reconstitution with an N-terminally truncated PsbP, which can bind to the PSII core without restoration of  $\text{Ca}^{2+}$  and  $\text{Cl}^-$  retention (36, 37), was also investigated. The results provide solid evidence that the PsbP protein induces the conformational changes in the protein moieties around the Mn cluster, suggesting that these conformational changes regulate the binding properties of  $\text{Ca}^{2+}$  and  $\text{Cl}^-$ .

## MATERIALS AND METHODS

Oxygen-evolving PSII membranes of spinach (38) were prepared as reported previously (39) and suspended in a Mes buffer at pH 6.0 (buffer A consisting of 40 mM Mes-NaOH, 400 mM sucrose, 5 mM NaCl, and 5 mM  $\text{CaCl}_2$ ). Depletion of PsbP and PsbQ was performed by NaCl washing (39, 40), in which the sample was incubated in a buffer containing 2 M NaCl

[40 mM Mes-NaOH, 400 mM sucrose, 5 mM  $\text{CaCl}_2$ , and 2 M NaCl (pH 6.5)] for 20 min on ice, followed by washing with the same buffer and then again with buffer A. PsbP, PsbQ, and PsbO depletion was performed by  $\text{CaCl}_2$  washing (39, 41) in a similar manner using a buffer containing 1 M  $\text{CaCl}_2$  [40 mM Mes-NaOH, 400 mM sucrose, 5 mM NaCl, and 1 M  $\text{CaCl}_2$  (pH 6.5)]. The depletion of extrinsic proteins by these treatments was confirmed by SDS–PAGE (Supporting Information, Figure S1).

Recombinant spinach PsbP was expressed in *Escherichia coli* [strain BL21(DE3)] cells and purified as described previously (42).  $\Delta 15$ -PsbP, in which the 15 N-terminal residues were truncated, was prepared as described previously (37). The [ $^{13}\text{C}$ ]PsbP protein, in which the carbon atoms were universally labeled with  $^{13}\text{C}$ , was prepared by culturing *E. coli* cells in a  $^{13}\text{C}$ -labeled bacterial growth medium [ $^{13}\text{C}$  Spectra 9 Medium,  $\geq 98$  at %  $^{13}\text{C}$  (Spectra Gases Inc., Columbia, MD)] followed by purification. Reconstitution of the PSII membranes with the PsbP protein was performed by adding the purified PsbP protein to the NaCl-washed PSII (0.5 mg of Chl/mL) in buffer A at a molar ratio of 3 per PSII reaction center, followed by incubation for 1 h on ice. For  $\Delta 15$ -PsbP, a higher molar ratio of 5 was used for reconstitution due to a slightly lower binding affinity (36, 37). The samples were then washed once with buffer A. The successful rebinding of PsbP and  $\Delta 15$ -PsbP to the NaCl-washed PSII membranes was confirmed by SDS–PAGE (Supporting Information, Figure S1).

For FTIR measurements, membrane samples were suspended in buffer A in the presence of 18 mM potassium ferrocyanide and 2 mM potassium ferricyanide and centrifuged at 170000g for 30 min, and the resulting pellet was sandwiched between two  $\text{BaF}_2$  plates (13 mm in diameter) (43). Here, ferricyanide acts as an exogenous electron acceptor and ferrocyanide is necessary for maintaining the redox potential sufficiently low to prevent oxidation of the non-heme iron (44). The sample temperature was adjusted to 250 K in a cryostat (Oxford DN1704).

Light-induced FTIR difference spectra upon the  $\text{S}_1 \rightarrow \text{S}_2$  transition (hereafter termed  $\text{S}_2/\text{S}_1$  difference spectra) were recorded using a Bruker IFS-66/S spectrophotometer equipped with an MCT detector (Infrared D316/8) at  $4\text{ cm}^{-1}$  resolution (43). Illumination was performed using a Q-switched Nd:YAG laser (Quanta-Ray GCR-130, 532 nm,  $\sim 7$  ns full width at half-maximum,  $\sim 7\text{ mJ pulse}^{-1}\text{ cm}^{-2}$  at the sample surface). Single-beam spectra (150 s scan) were recorded before and 10 s after single-flash illumination, providing a difference spectrum via subtraction of the initial spectrum from the one obtained after illumination. The 10 s interval after the flash was used to allow complete reoxidation of  $\text{Q}_\text{A}^-$  by ferricyanide. The measurements were repeated three to five times for each sample. The samples were warmed to 285 K to relax the  $\text{S}_2$  state and then cooled again to 250 K. One or two samples were used for measurements, and the obtained spectra were averaged.

FTIR spectra of the unlabeled and  $^{13}\text{C}$ -labeled PsbP proteins in Mes buffer [10 mM Mes and 10 mM NaCl (pH 6.0)] were recorded at room temperature. The PsbP solution ( $\sim 15\text{ mg/mL}$ ) was sandwiched between two  $\text{CaF}_2$  plates with a piece of aluminum foil as a spacer. A water band around  $1640\text{ cm}^{-1}$  was removed from the spectra by subtracting a buffer spectrum obtained in a similar manner.

## RESULTS

The  $\text{S}_2/\text{S}_1$  FTIR difference spectra of untreated, NaCl-washed,  $\text{CaCl}_2$ -washed, and NaCl-washed and then PsbP-reconstituted

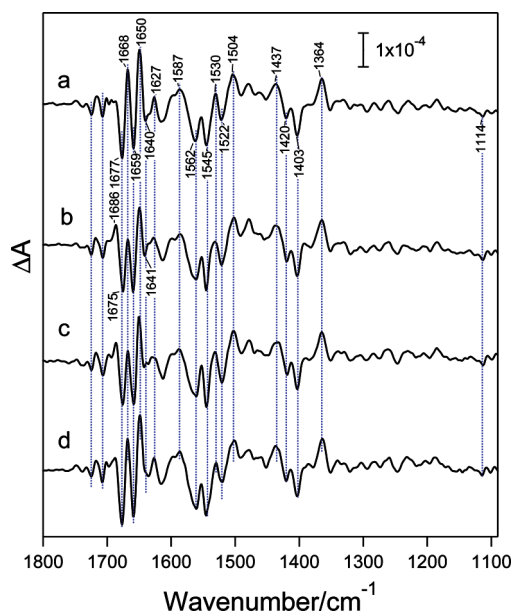


FIGURE 1: Light-induced  $S_2/S_1$  FTIR difference spectra of the OEC in PSII membranes from spinach: (a) untreated PSII, (b) NaCl-washed PSII, (c)  $\text{CaCl}_2$ -washed PSII, and (d) NaCl-washed, PsbP-reconstituted PSII. Samples contained ferricyanide as an exogenous electron acceptor, and a single flash illumination induced the  $S_1 \rightarrow S_2$  transition in the OEC. The sample temperature was 250 K.

PSII membranes from spinach are displayed in Figure 1. The  $S_2/S_1$  difference spectrum of untreated PSII membranes (Figure 1a) is identical to the one reported previously using the same spinach preparation (43) and similar to the spectra of cyanobacterial PSII core complexes (45–47). The bands in the  $S_2/S_1$  difference spectrum for untreated PSII were assigned on the basis of group frequencies and universal or amino acid-specific isotope substitutions (43, 45, 47, 48). Prominent bands in the 1700–1600  $\text{cm}^{-1}$  region arise from the amide I vibrations ( $\text{C}=\text{O}$  stretches of backbone amides) of polypeptide main chains, while the amide II bands (NH bend and CN stretch of backbone amides) of main chains and the asymmetric  $\text{COO}^-$  stretching bands of carboxylate groups overlap in the 1600–1500  $\text{cm}^{-1}$  region. Bands at 1450–1350  $\text{cm}^{-1}$  arise from symmetric  $\text{COO}^-$  stretching vibrations, and a small negative peak at 1114  $\text{cm}^{-1}$  was assigned to the CN stretching vibration of an imidazole group of His.

The appearance of several intense peaks in the amide I region (Figure 1a) reflects the conformational changes of distinct main chain regions around the Mn cluster. In addition, the presence of several bands in the symmetric  $\text{COO}^-$  region and one His peak is consistent with the X-ray crystallographic structure of the OEC (5–7), in which the Mn cluster is surrounded by five or six carboxylate groups from Asp, Glu, and the C-terminus, and a few imidazole groups from His. Some of these carboxylate and imidazole groups should function as ligands to the Mn and Ca ions, and others may be coupled to the Mn cluster through H-bonding or electrostatic interactions, although the details have not yet been resolved (33, 34).

Even when the PsbP and PsbQ proteins were depleted by NaCl washing (39, 40), the  $S_2/S_1$  difference spectrum (Figure 1b) exhibited overall features similar to those of the untreated sample (Figure 1a). In particular, the symmetric  $\text{COO}^-$  stretching bands in the 1450–1300  $\text{cm}^{-1}$  region and the His peak at 1114  $\text{cm}^{-1}$  were virtually unchanged, indicating that the ligand structure of the Mn cluster was not affected by PsbP and PsbQ depletion.

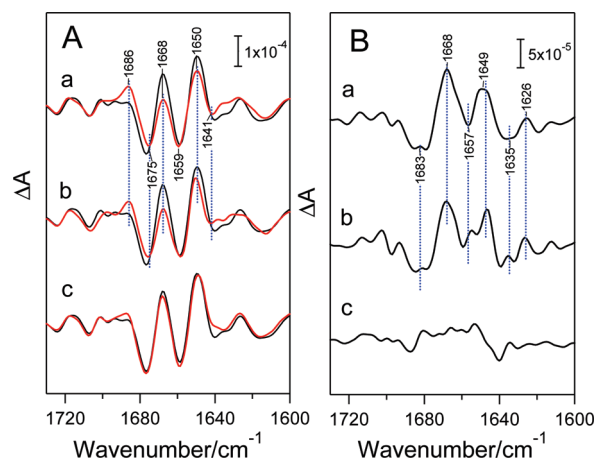


FIGURE 2: (A) Expanded spectra of the amide I region of the  $S_2/S_1$  FTIR difference spectra. The spectra of NaCl-washed PSII (a),  $\text{CaCl}_2$ -washed PSII (b), and NaCl-washed, PsbP-reconstituted PSII (c) (red lines) were compared with the spectrum of untreated PSII (black lines). (B) Double-difference spectra between the  $S_2/S_1$  spectra of salt-washed, PsbP-reconstituted PSII and untreated PSII: (a) untreated-minus-NaCl-washed PSII, (b) untreated-minus- $\text{CaCl}_2$ -washed PSII, and (c) untreated-minus-NaCl-washed, PsbP-reconstituted PSII.

In the amide I region (1700–1600  $\text{cm}^{-1}$ ), however, the spectral features clearly changed. Expanded spectra of this region are shown in Figure 2Aa. A new positive peak appeared at 1686  $\text{cm}^{-1}$ , and the intensity of the peak at 1668  $\text{cm}^{-1}$  decreased significantly. In addition, the intensity of the positive peak at 1650  $\text{cm}^{-1}$  decreased slightly and the negative peaks at 1677 and 1640  $\text{cm}^{-1}$  shifted to 1675 and 1641  $\text{cm}^{-1}$ , respectively.

These changes are expressed more clearly in an untreated-minus-NaCl-washed double-difference spectrum (Figure 2Ba), in which prominent peaks were observed at 1683, 1668, 1657, 1649, 1635, and 1626  $\text{cm}^{-1}$ . This double-difference spectrum did not exhibit appreciable peaks in the 1450–1100  $\text{cm}^{-1}$  region, where carboxylate and imidazole bands are present, whereas several medium peaks were observed at 1600–1500  $\text{cm}^{-1}$ , likely due to amide II vibrations coupled with the changes in the amide I bands (Supporting Information, Figure S2).

It should be noted that the PsbP- and PsbQ-depleted PSII sample contained 5 mM  $\text{CaCl}_2$  and 5 mM NaCl, and consequently,  $\text{Ca}^{2+}$  and  $\text{Cl}^-$  were not released from the OEC during sample preparation and measurement. In fact, the  $\text{Ca}^{2+}$ -depleted (43, 49) and  $\text{Cl}^-$ -depleted (50) PSII samples displayed  $S_2/S_1$  spectral features significantly different from those of Figure 1b. The  $S_2/S_1$  difference spectra of NaCl-washed PSII membranes reported previously by Kimura and co-workers (51, 52) exhibited amide I features similar to those in Figures 1b and 2Aa (red line).

The  $\text{CaCl}_2$ -washed PSII, in which PsbO was removed in addition to PsbP and PsbQ (39, 41), gave an  $S_2/S_1$  spectrum (Figures 1c) virtually identical to that of NaCl-washed PSII (Figure 1b). The carboxylate and His bands in the 1450–1100  $\text{cm}^{-1}$  region were unchanged from those of untreated PSII (Figure 1a), whereas amide I bands showed large changes very similar to those of the PsbP- and PsbQ-depleted PSII (Figure 2Ab,Bb). Indeed, a double-difference spectrum between the spectra of NaCl-washed and  $\text{CaCl}_2$ -washed PSII samples exhibited no appreciable bands (data not shown). Thus, no effect of further depletion of PsbO was observed in the  $S_2/S_1$  FTIR spectra.

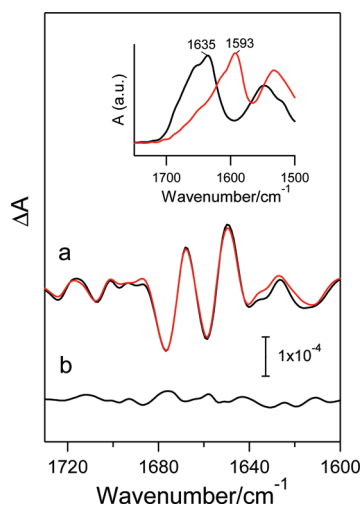


FIGURE 3: (a) Amide I region of the  $S_2/S_1$  FTIR difference spectrum of the NaCl-washed PSII membranes reconstituted with  $^{13}\text{C}$ -labeled PsbP (red line) compared with that of untreated PSII (black line). Measurement conditions were the same as those described in the legend of Figure 1. (b) Double-difference spectrum between the  $S_2/S_1$  spectra of  $^{13}\text{C}$ PsBP-reconstituted and untreated PSII (untreated-minus- $^{13}\text{C}$ PsBP-reconstituted PSII). The inset shows FTIR spectra of unlabeled (black line) and  $^{13}\text{C}$ -labeled (red line) PsbP in Mes buffer measured at room temperature. The spectral baseline was corrected by subtracting a buffer spectrum.

Figure 1d shows the  $S_2/S_1$  difference spectrum of NaCl-washed PSII membranes reconstituted with PsbP. This sample corresponds to PsbQ-depleted SPII membranes. This spectrum and the expansion of the amide I region (Figure 2Ac) showed that the amide I features perturbed by PsbP and PabQ depletion were mostly restored by reconstitution with PsbP, and the spectrum became similar to that of the untreated sample. The double-difference spectrum between this spectrum and the untreated spectrum (Figure 2Bc) also demonstrated the restoration of the spectral features.

These results indicate that depletion of the PsbP protein, but not the PsbO and PsbQ proteins, induced the perturbation in the conformational changes of proteins upon the  $S_1 \rightarrow S_2$  transition. The next question is whether the affected amide I changes can be attributed to the PsbP protein itself, or to the intrinsic membrane-spanning proteins of PSII. To address this question, NaCl-washed PSII membranes were reconstituted with universally  $^{13}\text{C}$ -labeled PsbP. The FTIR spectrum of the PsbP protein exhibited an amide I peak at  $1635\text{ cm}^{-1}$  (Figure 3, inset, black line), the frequency typical of the  $\beta$ -sheet structure (53, 54), consistent with the X-ray structure of PsbP (55) and the previous FTIR analysis (56). The universal  $^{13}\text{C}$  labeling of PsbP caused a downshift of the amide I band by  $42\text{ cm}^{-1}$ , resulting in a band at  $1593\text{ cm}^{-1}$  (Figure 3, inset, red line). Thus, if the conformational changes of PsbP are involved in the  $S_2/S_1$  FTIR spectrum, its amide I bands should exhibit large downshifts of  $\sim 40\text{ cm}^{-1}$ .

The amide I region of the  $S_2/S_1$  FTIR difference spectra of PSII membranes reconstituted with  $^{13}\text{C}$ PsBP is displayed in Figure 3a (red line). This spectrum is virtually identical to the spectrum of untreated PSII possessing unlabeled PsbP (Figure 3a, black line), which was confirmed by the almost flat double-difference spectrum (Figure 3b). This result indicates that none of the amide I bands in the  $S_2/S_1$  difference spectrum originate from the PsbP protein itself, and thus, the PsbP-induced amide I changes are attributed to the intrinsic proteins.

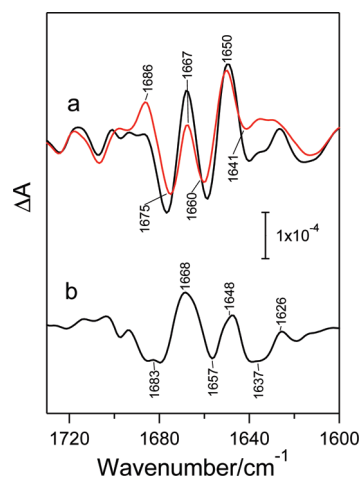


FIGURE 4: (a) Amide I region of the  $S_2/S_1$  FTIR difference spectrum of the NaCl-washed PSII membranes reconstituted with  $\Delta 15$ -PsbP (red line) compared with that of untreated PSII (black line). Measurement conditions were the same as those described in the legend of Figure 1. (b) Double-difference spectrum between the  $S_2/S_1$  spectra of  $\Delta 15$ -PsbP-reconstituted and untreated PSII (untreated-minus- $\Delta 15$ -PsbP-reconstituted PSII).

It has been shown that  $\Delta 15$ -PabP, in which the 15 N-terminal residues were truncated, can bind to NaCl-washed PSII membranes without functional recovery of  $\text{Ca}^{2+}$  and  $\text{Cl}^-$  retention (37). The  $S_2/S_1$  FTIR difference spectrum of NaCl-washed PSII membranes reconstituted with  $\Delta 15$ -PsbP (Figure 4a, red line) exhibited amide I features very similar to those of the NaCl-washed sample (Figure 2Aa). A double-difference spectrum with untreated PSII (Figure 4b) is also similar to that between NaCl-washed and untreated PSII samples (Figure 2Ba). To exclude the possibility that the 20 mM potassium ferrocyanide/ferricyanide added to the buffer to obtain the  $S_2/S_1$  spectrum released  $\Delta 15$ -PsbP with a binding affinity slightly lower than that of wild-type PsbP (36, 37),  $S_2Q_A^-/S_1Q_A$  spectra were measured without potassium ferrocyanide/ferricyanide. A comparison of the spectra between  $\Delta 15$ -PsbP-reconstituted and untreated PSII samples (Supporting Information, Figure S3a) reveals clear changes in the amide I region, and its double-difference spectrum (Figure S3b) is similar to the  $S_2/S_1$  difference spectra (Figure 4b). These results indicate that proper conformations of the OEC cannot be restored by the rebinding of  $\Delta 15$ -PsbP in contrast to wild-type PsbP.

## DISCUSSION

This FTIR analysis of the effects of extrinsic proteins on the OEC structure in spinach PSII membranes has demonstrated that the depletion of PsbP perturbs the protein conformations around the Mn cluster, as revealed by the clear changes in the amide I bands in the  $S_2/S_1$  difference spectra (Figure 2Aa,Ba), without appreciable changes in the ligand structures, which were monitored by symmetric carboxylate stretching bands ( $1450\text{--}1300\text{ cm}^{-1}$ ) and an imidazole CN stretching band ( $1114\text{ cm}^{-1}$ ) (Figure 1a). In contrast, the depletion of the other extrinsic proteins, PsbQ and PsbO, did not affect any OEC structures coupled to the  $S_1 \rightarrow S_2$  transition; the spectrum of PsbQ-depleted PSII, which was prepared by reconstitution of NaCl-washed PSII with recombinant PsbP, was virtually identical to the spectrum of untreated membranes (Figures 1d and 2Ac,Bc), and the depletion of the PsbP, PsbQ, and PsbO proteins by  $\text{CaCl}_2$  washing did not

result in further changes from the spectrum of the PsbP- and PsbQ-depleted PSII (Figures 1c and 2Ab,Bb).

The reconstitution with  $^{13}\text{C}$ -labeled PsbP proved that the amide I bands perturbed by PsbP depletion originated not from the PsbP protein itself but from the intrinsic core proteins (Figure 3). Because neither PsbQ nor PsbO affects the amide I bands, this indicates that the  $S_1 \rightarrow S_2$  transition induces protein conformational changes only in the intrinsic proteins, and the structure of none of the three extrinsic proteins is affected by this reaction. The presence of several peaks observed over the range of the amide I region ( $1700\text{--}1600\text{ cm}^{-1}$ ) indicates that several parts of the main chains are involved in the conformational changes. A major contribution of the acceptor side domain is unlikely because the donor side ( $S_2/S_1$ ) and acceptor side ( $Q_A^-/Q_A$ ,  $Q_B^-/Q_B$ , and  $\text{Fe}^{2+}/\text{Fe}^{3+}$ ) FTIR signals can be treated independently to reproduce or be calculated from the difference spectra of corresponding charge-separated states (43, 44, 51, 57). Thus, the primary candidates are the helical and loop regions of the D1 and CP43 proteins that include amino acid residues that provide ligands to the Mn cluster or are located nearby: the C-terminal loop of D1 including D1-Ala344, D1-Asp342, D1-His337, D1-Glu333, and D1-His332; the CD helix of D1 including D1-Glu189; the loop region of D1 between the C and CD helices including D1-Asp170; and the short  $3_{10}$ -helix of CP43 including CP43-Glu354 and CP43-Arg357 (5–7). The C-terminal helical region of D2 including D2-Lys317, which interacts with  $\text{Cl}^-$  (7, 9), could also be a candidate. According to the general criteria (53, 54), the peaks at  $1660\text{--}1650\text{ cm}^{-1}$  (Figure 1a) can be attributed to the  $\alpha$ -helical chains, and those around  $1665\text{ cm}^{-1}$  may arise from the  $3_{10}$ -helix. Although the peaks at  $1700\text{--}1660$  and  $1640\text{--}1620\text{ cm}^{-1}$  are usually assigned to turns and  $\beta$ -strands, the bands in these regions might arise mainly from the loop regions that have undefined interactions of amide groups. Some of these main chain portions are affected by the PsbP interaction, because PsbP-induced changes also resulted in several peaks over the amide I region (Figure 2Ba). The conformational changes by PsbP depletion could be related to the previous observation of a parallel polarization multiline EPR signal of the  $S_1$  state in PsbP- and PsbQ-depleted PSII from spinach (58). However, the observation that removal of all three extrinsic proteins did not induce this signal (58) is inconsistent with these FTIR results that the NaCl- and  $\text{CaCl}_2$ -washed PSII samples showed no appreciable differences (Figure 2Aa,b,Ba,b). Thus, the effect of PsbP and PsbQ depletion detected in the EPR signal may have an origin different from that detected by FTIR.

The PsbP-induced conformational changes around the Mn cluster are caused by the interaction of its N-terminal region; reconstitution with  $\Delta 15$ -PsbP, which lacks the 15 N-terminal residues, did not restore the conformations (Figure 4), in contrast to the wild-type PsbP (Figures 1d and 2Ac,Bc). This result correlates well with the previous observation that reconstitution with  $\Delta 15$ -PsbP did not restore the PsbP function of  $\text{Ca}^{2+}$  and  $\text{Cl}^-$  retention (37). Thus, the conformational changes of the OEC induced by the interaction of the N-terminal region of PsbP likely alter the binding properties of  $\text{Ca}^{2+}$  and  $\text{Cl}^-$  to prevent their dissociation.

The importance of the N-terminal region of PsbP in the interaction with the OEC is consistent with the fact that the structure of this region was not determined in the X-ray structure of the PsbP protein (55). The N-terminal region probably has a flexible structure in free PsbP and exhibits a fixed structure like a hook when interacting with a certain part of the intrinsic proteins

to maintain the proper OEC conformation. This hook may work as a switch to shift the OEC conformation from a low to high level of  $\text{Ca}^{2+}$  and  $\text{Cl}^-$  retention ability. It has been suggested that positively charged lysyl residues in this region (Lys11, Lys13, and Lys14) are involved in the interactions with PSII proteins (59) and  $\text{Ca}^{2+}$  and  $\text{Cl}^-$  retention (16, 37). Some acidic residues of the intrinsic proteins may be the counterparts of these interactions, although they have not yet been identified. The direct interaction of PsbP with the PSII core proteins is consistent with the location of PsbP in the PSII complexes predicted by an analysis of the electron cryomicroscopic structure (18) using the X-ray crystallographic information for the cyanobacterial PSII core complex (5) and plant PsbP (55) and PsbQ (60) proteins; it seemed to interact with the loops of CP43 and possibly with the C-terminus of the D1 protein.

The absence of the effect of PsbQ on the OEC structure in contrast to the strong coupling of PsbP with the OEC is consistent with the minor role of PsbQ in  $\text{Ca}^{2+}$  and  $\text{Cl}^-$  retention observed in *in vitro* experiments (12) and the lack of effect of its downregulation by RNAi on the growth of tobacco (27) and *Arabidopsis*, at least under normal light conditions (29). It is likely that PsbQ interacts with PsbP and stabilizes its interaction with the intrinsic proteins. In contrast, it was surprising that the PsbO protein, which binds more strongly to the PSII core proteins than PsbP and plays a significant role in the stabilization of the Mn cluster (12, 13), did not influence the OEC structure, at least when PsbP was absent. This FTIR result indicates that the molecular mechanism underlying the PsbO function is different from that of PsbP. PsbO may act mainly as a barrier to block the access of extrinsic reductants to the Mn cluster and the release of  $\text{Ca}^{2+}$  and  $\text{Cl}^-$  from the OEC without directly affecting the OEC structure. However, the possibility that PsbO perturbs the conformations of the protein moieties near the Mn cluster that are unaffected by the  $S_1 \rightarrow S_2$  transition and is thereby undetectable in FTIR spectra cannot be excluded. Another possibility is that structural changes in PsbO induced by PsbP binding perturb the OEC conformation. It should be noted that our result showing the absence of PsbO bands in the  $S_2/S_1$  difference spectrum is at odds with a previous study by Barry and co-workers (61), in which they observed changes in the  $S_2Q_A^-/S_1Q_A$  FTIR difference spectrum upon rebinding of  $^{13}\text{C}$ -labeled PsbO. However, the  $S_2Q_A^-/S_1Q_A$  spectra used in their analysis (61) did not resemble any of the  $S_2Q_A^-/S_1Q_A$  (57, 62–64),  $S_2/S_1$  (43, 46, 51, 63), or  $Q_A^-/Q_A$  (51, 64–66) difference spectra obtained by several other groups and were even different from the  $S_2Q_A^-/S_1Q_A$  spectrum of their own group reported later (67). These inconsistencies most likely arise from a large contribution of artifact signals to their spectra (this discrepancy has been discussed in detail in refs (65) and (68)). Thus, the conclusion reported by Barry and co-workers (61) on the PsbO effect was inferred from questionable experimental data.

The results of this FTIR study are summarized in the schematic in Figure 5. PsbP has an N-terminal hook that interacts with the intrinsic PSII proteins on the luminal side (Figure 5a). Upon PsbP depletion, together with PsbQ, this hook becomes detached, triggering the conformational changes around the Mn cluster that weaken the  $\text{Ca}^{2+}$  and  $\text{Cl}^-$  retention ability (Figure 5b). Further depletion of PsbO does not influence the conformation of the OEC (Figure 5c). Upon reconstitution with PsbP, but still in the absence of PsbQ, the interaction of the PsbP hook restores the protein conformations of the OEC (Figure 5d). However, if the N-terminal hook is truncated, this  $\Delta 15$ -PsbP

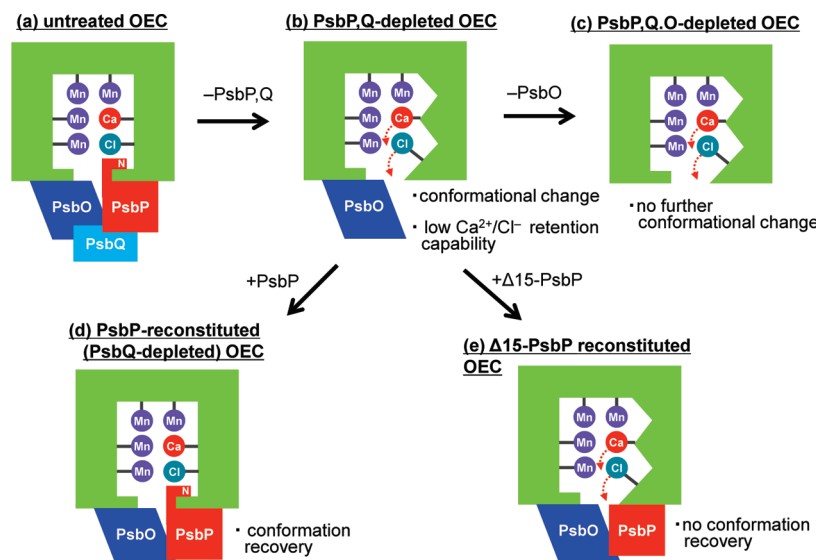


FIGURE 5: Schematic view of the relationships among the extrinsic proteins (PsbQ, PsbP, and PsbO), the OEC conformations, and the  $\text{Ca}^{2+}$  and  $\text{Cl}^-$  retention ability, obtained in our FTIR study. See the text for details.

protein binds to the PSII proteins but does not restore the protein conformation as well as the  $\text{Ca}^{2+}$  and  $\text{Cl}^-$  retention ability (Figure 5e).

In conclusion, this FTIR study provides solid evidence that binding of the PsbP protein influences the protein conformations around the Mn cluster, which probably improves the  $\text{Ca}^{2+}$  and  $\text{Cl}^-$  retention ability. Thus, PsbP is directly coupled to the OEC structure and regulates its stability. An intriguing question is whether cyanobacteria already had a similar mechanism for regulating the  $\text{Ca}^{2+}$  and  $\text{Cl}^-$  retention by using the PabV or PsbU protein or whether this regulation mechanism developed due to the appearance of PsbP during the evolutionary process. This could be a clue to understanding the extensive changes in extrinsic proteins during evolution from cyanobacteria to higher plants (12–15). Further FTIR studies using PSII preparations from other types of organisms might answer this question.

#### SUPPORTING INFORMATION AVAILABLE

SDS–PAGE analysis of PSII samples, the 1800–1100  $\text{cm}^{-1}$  region of the double difference spectra between the salt-washed/PsbP-reconstituted PSII and untreated PSII, and  $\text{S}_2\text{QA}^-/\text{S}_1\text{QA}$  FTIR difference spectra of untreated and NaCl-washed, Δ15-PsbP-reconstituted PSII membranes. This material is available free of charge via the Internet at <http://pubs.acs.org>.

#### REFERENCES

- Debus, R. J. (1992) The manganese and calcium ions of photosynthetic oxygen evolution. *Biochim. Biophys. Acta* 1102, 269–352.
- Hillier, W., and Messinger, J. (2005) Mechanism of photosynthetic oxygen production. In *Photosystem II: The Light-Driven Water: Plastoquinone Oxidoreductase* (Wydrzynski, T., and Satoh, K., Eds.) pp 567–608, Springer, Dordrecht, The Netherlands.
- McEvoy, J. P., and Brudvig, G. W. (2006) Water-splitting chemistry of photosystem II. *Chem. Rev.* 106, 4455–4483.
- Renger, G. (2007) Oxidative photosynthetic water splitting: Energetics, kinetics and mechanism. *Photosynth. Res.* 92, 407–425.
- Ferreira, K. N., Iverson, T. M., Maghlaoui, K., Barber, J., and Iwata, S. (2004) Architecture of the photosynthetic oxygen-evolving center. *Science* 303, 1831–1838.
- Loll, B., Kern, J., Saenger, W., Zouni, A., and Biesiadka, J. (2005) Towards complete cofactor arrangement in the 3.0 Å resolution structure of photosystem II. *Nature* 438, 1040–1044.
- Guskov, A., Kern, J., Gabdulkhakov, A., Broser, M., Zouni, A., and Saenger, W. (2009) Cyanobacterial photosystem II at 2.9-Å resolution and the role of quinones, lipids, channels and chloride. *Nat. Struct. Mol. Biol.* 16, 334–342.
- Yano, J., Kern, J., Sauer, K., Latimer, M. J., Pushkar, Y., Biesiadka, J., Loll, B., Saenger, W., Messinger, J., Zouni, A., and Yachandra, V. K. (2006) Where water is oxidized to dioxygen: Structure of the photosynthetic  $\text{Mn}_4\text{Ca}$  cluster. *Science* 314, 821–825.
- Murray, J. W., Maghlaoui, K., Kargul, J., Ishida, N., Lai, T.-L., Rutherford, A. W., Sugiura, M., Boussac, A., and Barber, J. (2008) X-ray crystallography identifies two chloride binding sites in the oxygen evolving centre of Photosystem II. *Energy Environ. Sci.* 1, 161–166.
- Yano, J., Kern, J., Irrgang, K. D., Latimer, M. J., Bergmann, U., Glatzel, P., Pushkar, Y., Biesiadka, J., Loll, B., Sauer, K., Messinger, J., Zouni, A., and Yachandra, V. K. (2005) X-ray damage to the  $\text{Mn}_4\text{Ca}$  complex in single crystals of photosystem II: A case study for metalloprotein crystallography. *Proc. Natl. Acad. Sci. U.S.A.* 102, 12047–12052.
- Grabolle, M., Haumann, M., Muller, C., Liebisch, P., and Dau, H. (2006) Rapid loss of structural motifs in the manganese complex of oxygenic photosynthesis by X-ray irradiation at 10–300 K. *J. Biol. Chem.* 281, 4580–4588.
- Seidler, A. (1996) The extrinsic polypeptides of Photosystem II. *Biochim. Biophys. Acta* 1277, 35–60.
- Bricker, T. M., and Burnap, R. L. (2005) The extrinsic proteins of photosystem II. In *Photosystem II: The Light-Driven Water: Plastoquinone Oxidoreductase* (Wydrzynski, T., and Satoh, K., Eds.) pp 95–120, Springer, Dordrecht, The Netherlands.
- Roose, J. L., Wegener, K. M., and Pakrasi, H. B. (2007) The extrinsic proteins of photosystem II. *Photosynth. Res.* 92, 369–387.
- Enami, I., Okumura, A., Nagao, R., Suzuki, T., Iwai, M., and Shen, J.-R. (2008) Structures and functions of the extrinsic proteins of photosystem II from different species. *Photosynth. Res.* 98, 349–363.
- Ifuku, K., Ishihara, S., Shimamoto, R., Ido, K., and Sato, F. (2008) Structure, function, and evolution of the PsbP protein family in higher plants. *Photosynth. Res.* 98, 427–437.
- Miyao, M., Murata, N., Lavorel, J., Maisonneuve, B., Boussac, A., and Etienne, A. L. (1987) Effect of the 33 kDa protein on the S-state transitions in photosynthetic oxygen evolution. *Biochim. Biophys. Acta* 890, 151–159.
- Nield, J., and Barber, J. (2006) Refinement of the structural model for the Photosystem II supercomplex of higher plants. *Biochim. Biophys. Acta* 1757, 353–361.
- Miyao, M., and Murata, N. (1983) Partial reconstitution of the photosynthetic oxygen evolution system by rebinding of the 33-kDa polypeptide. *FEBS Lett.* 164, 375–378.
- Miyao, M., and Murata, N. (1983) Partial disintegration and reconstitution of the photosynthetic oxygen evolution system. Binding of 24 kDa and 18 kDa polypeptides. *Biochim. Biophys. Acta* 725, 87–93.

- (21) Adelroth, P., Lindberg, K., and Andréasson, L. E. (1995) Studies of  $\text{Ca}^{2+}$  binding in spinach photosystem II using  $^{45}\text{Ca}^{2+}$ . *Biochemistry* 34, 9021–9027.
- (22) Wincencjusz, H., Yocum, C. F., and van Gorkom, H. J. (1998) S-state dependence of chloride binding affinities and exchange dynamics in the intact and polypeptide-depleted  $\text{O}_2$  evolving complex of photosystem II. *Biochemistry* 37, 8595–8604.
- (23) Ghanotakis, D. F., Babcock, G. T., and Yocum, C. F. (1984) Calcium reconstitutes high rates of oxygen evolution in polypeptide depleted Photosystem II preparations. *FEBS Lett.* 167, 127–130.
- (24) Miyao, M., and Murata, N. (1984) Calcium ions can be substituted for the 24-kDa polypeptide in photosynthetic oxygen evolution. *FEBS Lett.* 168, 118–120.
- (25) Boussac, A., and Rutherford, A. W. (1988) Nature of the inhibition of the oxygen-evolving enzyme of photosystem II induced by sodium chloride washing and reversed by the addition of  $\text{Ca}^{2+}$  or  $\text{Sr}^{2+}$ . *Biochemistry* 27, 3476–3483.
- (26) Ghanotakis, D. F., Topper, J. N., and Yocum, C. F. (1984) Structural organization of the oxidizing side of photosystem II. Exogenous reductants reduce and destroy the Mn-complex in photosystems II membranes depleted of the 17 and 23 kDa polypeptides. *Biochim. Biophys. Acta* 767, 524–531.
- (27) Ifuku, K., Yamamoto, Y., Ono, T., Ishihara, S., and Sato, F. (2005) PsbP protein, but not PsbQ protein, is essential for the regulation and stabilization of photosystem II in higher plants. *Plant Physiol.* 139, 1175–1184.
- (28) Yi, X. P., Hargett, S. R., Liu, H. J., Frankel, L. K., and Bricker, T. M. (2007) The PsbP protein is required for photosystem II complex assembly/stability and photoautotrophy in *Arabidopsis thaliana*. *J. Biol. Chem.* 282, 24833–24841.
- (29) Yi, X. P., Hargett, S. R., Frankel, L. K., and Bricker, T. M. (2006) The PsbQ protein is required in *Arabidopsis* for photosystem II assembly/stability and photoautotrophy under low light conditions. *J. Biol. Chem.* 281, 26260–26267.
- (30) Chu, H.-A., Hillier, W., Law, N. A., and Babcock, G. T. (2001) Vibrational spectroscopy of the oxygen-evolving complex and of manganese model compounds. *Biochim. Biophys. Acta* 1503, 69–82.
- (31) Noguchi, T., and Berthomieu, C. (2005) Molecular analysis by vibrational spectroscopy. In *Photosystem II: The Light-Driven Water:Plastoquinone Oxidoreductase* (Wydrzynski, T., and Satoh, K., Eds.) pp 367–387, Springer, Dordrecht, The Netherlands.
- (32) Noguchi, T. (2007) Light-induced FTIR difference spectroscopy as a powerful tool toward understanding the molecular mechanism of photosynthetic oxygen evolution. *Photosynth. Res.* 91, 59–69.
- (33) Noguchi, T. (2008) Fourier transform infrared analysis of the photosynthetic oxygen-evolving center. *Coord. Chem. Rev.* 252, 336–346.
- (34) Debus, R. J. (2008) Protein ligation of the photosynthetic oxygen-evolving center. *Coord. Chem. Rev.* 252, 244–258.
- (35) Noguchi, T. (2008) FTIR detection of water reactions in the oxygen-evolving center of photosystem II. *Philos. Trans. R. Soc. London, Ser. B* 363, 1189–1195.
- (36) Ifuku, K., and Sato, F. (2002) A truncated mutant of the extrinsic 23-kDa protein that absolutely requires the extrinsic 17-kDa protein for  $\text{Ca}^{2+}$  retention in photosystem II. *Plant Cell Physiol.* 43, 1244–1249.
- (37) Ifuku, K., Nakatsu, T., Shimamoto, R., Yamamoto, Y., Ishihara, S., Kato, H., and Sato, F. (2005) Structure and function of the PsbP protein of Photosystem II from higher plants. *Photosynth. Res.* 84, 251–255.
- (38) Berthold, D. A., Babcock, G. T., and Yocum, C. F. (1981) A highly resolved, oxygen-evolving photosystem II preparation from spinach thylakoid membranes. EPR and electron-transport properties. *FEBS Lett.* 134, 231–234.
- (39) Ono, T., and Inoue, Y. (1986) Effects of removal and reconstitution of the extrinsic 33, 24 and 16 kDa proteins on flash oxygen yield in photosystem II particles. *Biochim. Biophys. Acta* 850, 380–389.
- (40) Akerlund, H.-E., Jansson, C., and Andersson, B. (1982) Reconstitution of photosynthetic water splitting in inside-out thylakoid vesicles and identification of a participating polypeptide. *Biochim. Biophys. Acta* 681, 1–10.
- (41) Ono, T., and Inoue, Y. (1983) Mn-preserving extraction of 33-, 24- and 16-kDa proteins from  $\text{O}_2$ -evolving PS II particles by divalent salt-washing. *FEBS Lett.* 164, 255–260.
- (42) Ifuku, K., and Sato, F. (2001) Importance of the N-terminal sequence of the extrinsic 23 kDa polypeptide in Photosystem II in ion retention in oxygen evolution. *Biochim. Biophys. Acta* 1546, 196–204.
- (43) Noguchi, T., Ono, T., and Inoue, Y. (1995) Direct detection of a carboxylate bridge between Mn and  $\text{Ca}^{2+}$  in the photosynthetic oxygen-evolving center by means of Fourier transform infrared spectroscopy. *Biochim. Biophys. Acta* 1228, 189–200.
- (44) Noguchi, T., and Inoue, Y. (1995) Identification of Fourier-transform infrared signals from the non-heme iron in photosystem II. *J. Biochem.* 118, 9–12.
- (45) Noguchi, T., and Sugiura, M. (2003) Analysis of flash-induced FTIR difference spectra of the S-state cycle in the photosynthetic water-oxidizing complex by uniform  $^{15}\text{N}$  and  $^{13}\text{C}$  isotope labeling. *Biochemistry* 42, 6035–6042.
- (46) Chu, H.-A., Hillier, W., and Debus, R. J. (2004) Evidence that the C-terminus of the D1 polypeptide of photosystem II is ligated to the manganese ion that undergoes oxidation during the  $\text{S}_1$  to  $\text{S}_2$  transition: An isotope-edited FTIR study. *Biochemistry* 43, 3152–3166.
- (47) Yamanari, T., Kimura, Y., Mizusawa, N., Ishii, A., and Ono, T. (2004) Mid- to low-frequency Fourier transform infrared spectra of S-state cycle for photosynthetic water oxidation in *Synechocystis* sp PCC 6803. *Biochemistry* 43, 7479–7490.
- (48) Noguchi, T., Inoue, Y., and Tang, X.-S. (1999) Structure of a histidine ligand in the photosynthetic oxygen-evolving complex as studied by light-induced Fourier transform infrared difference spectroscopy. *Biochemistry* 38, 10187–10195.
- (49) Taguchi, Y., and Noguchi, T. (2007) Drastic changes in the ligand structure of the oxygen-evolving Mn cluster upon  $\text{Ca}^{2+}$  depletion as revealed by FTIR difference spectroscopy. *Biochim. Biophys. Acta* 1767, 535–540.
- (50) Hasegawa, K., Kimura, Y., and Ono, T. (2002) Chloride cofactor in the photosynthetic oxygen-evolving complex studied by Fourier transform infrared spectroscopy. *Biochemistry* 41, 13839–13850.
- (51) Kimura, Y., and Ono, T. (2001) Chelator-induced disappearance of carboxylate stretching vibrational modes in  $\text{S}_2/\text{S}_1$  FTIR spectrum in oxygen-evolving complex of photosystem II. *Biochemistry* 40, 14061–14068.
- (52) Kimura, Y., Hasegawa, K., and Ono, T. (2002) Characteristic changes of the  $\text{S}_2/\text{S}_1$  difference FTIR spectrum induced by  $\text{Ca}^{2+}$  depletion and metal cation substitution in the photosynthetic oxygen-evolving complex. *Biochemistry* 41, 5844–5853.
- (53) Byler, D. M., and Susi, H. (1986) Examination of the secondary structure of proteins by deconvolved FTIR spectra. *Biopolymers* 25, 469–487.
- (54) Surewicz, W. K., and Mantsch, H. H. (1988) New insight into protein secondary structure from resolution-enhanced infrared spectra. *Biochim. Biophys. Acta* 952, 115–130.
- (55) Ifuku, K., Nakatsu, T., Kato, H., and Sato, F. (2004) Crystal structure of the PsbP protein of photosystem II from *Nicotiana tabacum*. *EMBO Rep.* 5, 362–367.
- (56) Zhang, H., Ishikawa, Y., Yamamoto, Y., and Carpentier, R. (1998) Secondary structure and thermal stability of the extrinsic 23 kDa protein of photosystem II studied by Fourier transform infrared spectroscopy. *FEBS Lett.* 426, 347–351.
- (57) Zhang, H., Fischer, G., and Wydrzynski, T. (1998) Room-temperature vibrational difference spectrum for  $\text{S}_2\text{Q}_\text{B}^-/\text{S}_1\text{Q}_\text{B}$  of photosystem II determined by time-resolved Fourier transform infrared spectroscopy. *Biochemistry* 37, 5511–5517.
- (58) Campbell, K. A., Gregor, W., Pham, D. P., Peloquin, J. M., Debus, R. J., and Britt, R. D. (1998) The 23 and 17 kDa extrinsic proteins of photosystem II modulate the magnetic properties of the  $\text{S}_1$ -state manganese cluster. *Biochemistry* 37, 5039–5045.
- (59) Tohri, A., Dohmae, N., Suzuki, T., Ohta, H., Inoue, Y., and Enami, I. (2004) Identification of domains on the extrinsic 23 kDa protein possibly involved in electrostatic interaction with the extrinsic 33 kDa protein in spinach photosystem II. *Eur. J. Biochem.* 271, 962–971.
- (60) Calderone, V., Trabucco, M., Vujcic, A., Battistutta, R., Giacometti, G. M., Andreucci, F., Barbato, R., and Zanotti, G. (2003) Crystal structure of the PsbQ protein of photosystem II from higher plants. *EMBO Rep.* 4, 900–905.
- (61) Hutchison, R. S., Steenhuis, J. J., Yocum, C. F., Razeghifard, M. R., and Barry, B. A. (1999) Deprotonation of the 33-kDa, extrinsic, manganese-stabilizing subunit accompanies photooxidation of manganese in photosystem II. *J. Biol. Chem.* 274, 31987–31995.
- (62) Noguchi, T., Ono, T., and Inoue, Y. (1992) Detection of structural changes upon  $\text{S}_1$ -to- $\text{S}_2$  transition in the oxygen-evolving manganese cluster in photosystem II by light-induced Fourier transform infrared difference spectroscopy. *Biochemistry* 31, 5953–5956.
- (63) Chu, H.-A., Gardner, M. T., O'Brien, J. P., and Babcock, G. T. (1999) Low-frequency Fourier transform infrared spectroscopy of

- the oxygen-evolving and quinone acceptor complexes in photosystem II. *Biochemistry* 38, 4533–4541.
- (64) Remy, A., Niklas, J., Kuhl, H., Kellers, P., Schott, T., Rögner, M., and Gerwert, K. (2004) FTIR spectroscopy shows structural similarities between photosystems II from cyanobacteria and spinach. *Eur. J. Biochem.* 271, 563–567.
- (65) Hienerwadel, R., Boussac, A., Breton, J., and Berthomieu, C. (1996) Fourier transform infrared difference study of Tyrosine<sub>D</sub> oxidation and plastoquinone Q<sub>A</sub> reduction in photosystem II. *Biochemistry* 35, 15447–15460.
- (66) Noguchi, T., Kurreck, J., Inoue, Y., and Renger, G. (1999) Comparative FTIR analysis of the microenvironment of Q<sub>A</sub><sup>•-</sup> in cyanide-treated, high pH-treated and iron-depleted photosystem II membrane fragments. *Biochemistry* 38, 4846–4852.
- (67) Halverson, K. M., and Barry, B. A. (2003) Evidence for spontaneous structural changes in a dark-adapted state of photosystem II. *Biophys. J.* 85, 2581–2588.
- (68) Onoda, K., Mino, H., Inoue, Y., and Noguchi, T. (2000) An FTIR study on the structure of the oxygen-evolving Mn-cluster of photosystem II in different spin forms of the S<sub>2</sub> state. *Photosynth. Res.* 63, 47–57.